Journal of Marine Systems 242 (2024) 103938

Contents lists available at ScienceDirect

Journal of Marine Systems

journal homepage: www.elsevier.com/locate/jmarsys

Effect of circulation at early life stages of European anchovy in the Bay of Biscay from observational data and a Lagrangian approach

Ivan Manso-Narvarte [a,*], Ainhoa Caballero [a], Ismael Hernández-Carrasco [b], Alejandro Orfila [b], María Santos Mocoroa [a], Unai Cotano [a], Gabriel Jordà [c], Amandine Declerck [d], Matthias Delpey [d], Anna Rubio [a]

[a] Marine Research, AZTI, Pasaia, Spain
[b] Mediterranean Institute for Advanced Studies, IMEDEA (CSIC-UIB), Esporles, Spain
[c] Baleares Oceanographic Centre, Spanish Institute of Oceanography (IEO), Palma, Spain
[d] Center Rivages Pro Tech, SUEZ France Smart & Environmental Solutions, Bidart, France

ARTICLE INFO

Keywords:
Lagrangian diagnostics
Coastal circulation
Transport processes
Fish larvae
HF radar
Multiplatform observations
3D data reconstruction
Lagrangian Coherent Structures
Bay of Biscay

ABSTRACT

Coastal circulation influences the distribution of European anchovy (*Engraulis encrasicolus*) at early life stages (ELS) in the Bay of Biscay (BoB). However, how this happens is not yet fully understood. In this work, further insight is provided by performing Lagrangian diagnostics based on observations of ELS anchovies' initial distributions and currents. Surface diagnostics were obtained by using high-frequency radar (HFR) currents and were applied to analyse multiyear variability and detect the coastal processes that affect the distribution. Since ELS anchovies are also located at subsurface levels, subsurface diagnostics were obtained by using currents reconstructed from HFR and ADCP observations with a reduced order optimal interpolation (ROOI) method. The analyses included transport computations as well as the analysis of flow properties by Lagrangian Coherent Structures and chlorophyll-a satellite images.

Results suggest that ELS anchovies are mostly retained over the shelf and slope, and that transport patterns highly vary across different periods. Mesoscale structures such as eddies, fronts and along-slope currents within the slope and the Capbreton canyon area, as well as strong and persistent winds, could significantly impact the distribution of ELS anchovies. In some periods, the resulting distribution might be due to a combination of these processes. Circulation can also play a key role in ELS anchovy aggregation within short time scales (20 days). This work showcases the potential of observation-based approaches and emphasizes the relevance of coastal observatories for integrated studies.

1. Introduction

Coastal transport and retention result from the multi-scale interaction of large-scale and local circulation processes and show high spatiotemporal variability. They are crucial from an environmental and ecological perspective as they can strongly affect the fate of pollutants such as floating marine litter (e.g. Declerck et al., 2019; Ruiz et al., 2020; Van Sebille et al., 2020) and oil spills (e.g. Abascal et al., 2010; Otero et al., 2014; Sebastiao and Soares, 2006), as well as the biological component of the ecosystem. They modulate the distribution of phytoplankton and nutrient-rich coastal waters (e.g. Campbell et al., 2013; Moore et al., 2007; Rubio et al., 2018), and drastically impact the survival rates and population dynamics of fish larvae (e.g. Díaz-Barroso et al., 2022; Hidalgo et al., 2019; Sciascia et al., 2018).

They also affect the distribution at early life stages (ELS, i.e. egg and larvae stages) of different fish species (e.g. Mullaney and Suthers, 2013; Sabatés et al., 2007a, 2007b; Somarakis and Nikolioudakis, 2007), as occurs with the European anchovy (*Engraulis encrasicolus*) in the Bay of Biscay (BoB). The spawning of this species peaks around May–June and the main spawning areas are the fronts of Gironde and Adour River plumes and to a lesser extent the shelf-break areas nearby (Fig. 1b) (Motos et al., 1996). Eggs are mainly located in the upper water column (Boyra et al., 2003; Coombs et al., 2004), however, to the authors' knowledge, published observations of larvae vertical distributions are missing in the area. Several authors have pointed out that transport plays a critical role in their recruitment through changes in the food

* Corresponding author.
E-mail address: imanso@azti.es (I. Manso-Narvarte).

https://doi.org/10.1016/j.jmarsys.2023.103938
Received 5 January 2023; Received in revised form 29 September 2023; Accepted 8 October 2023
Available online 11 October 2023

availability and risk of predation (e.g. Bachiller et al., 2013; Cotano et al., 2008; Irigoien et al., 2008). Vessel-based observations have shown a seasonal southwestwards transport from the shelf to the shelf-break, slope and adjacent open ocean areas driven by the spring northeasterly winds. Then, they remain in those areas and later return to the shelf as mobile juveniles (Boyra et al., 2016; Cotano et al., 2008; Irigoien et al., 2008; Uriarte et al., 2001). In addition to the coast acting as a barrier, eddies were suggested to restrict the offshore transport of ELS anchovies (Irigoien et al., 2008).

The above-mentioned studies provided valuable information on transport patterns on a seasonal scale. At smaller spatiotemporal scales, several studies have analysed the transport of ELS anchovies from a Lagrangian approach (i.e. monitoring the motion of fluid parcels and their properties). These studies used high-resolution modelled currents with spatial resolutions ranging from 1 to 8 km and temporal resolutions ranging from 0.25 to 6 h. Allain et al. (2001, 2007) computed transports over three years, using averaged modelled currents over the upper 30 m and for computation periods extending up to 100 days, surpassing the passive period of anchovies (Irigoien et al., 2008). In Ferrer et al. (2004), transports were computed over three different years, forced by modelled currents at 5 m and for computation periods that ranged from 14 days to 4 months. Huret et al. (2010) tested different computation configurations in terms of initial positions, integration periods and vertical movements, for spawning periods from 1996 to 2007. The results of Ferrer et al. (2004) suggested limited dispersal of ELS anchovies towards the open ocean, while Allain et al. (2001, 2007) and Huret et al. (2010) suggested a stronger offshore transport, varying by spawning location and period considered. Despite the different transport patterns observed in these studies, none of them provided a comprehensive understanding of their variability throughout multiple years or how various coastal processes affected them.

The extensive historical datasets existing today in the southeastern Bay of Biscay (SE-BoB, Fig. 1a) allow performing new Lagrangian diagnostics using observational data. The SE-BoB is characterised by an abrupt change in the orientation of the coast and the presence of the steep Capbreton submarine canyon, which separates the narrower Spanish shelf from the wider French shelf (Fig. 1b). The Iberian Poleward slope Current (hereinafter IPC) plays a significant role in the along-slope transport. It strongly flows poleward in late autumn and winter, while it presents a weaker and more variable equatorward flow in summer (Charria et al., 2013; Solabarrieta et al., 2014). The effect of wind adds complexity to this seasonality (González et al., 2004; Solabarrieta et al., 2015) with prevailing southwesterlies in autumn and winter reinforcing the winter poleward flow, and northeasterlies in spring and summer contributing to a weaker and highly variable equatorward flow. On the shelf, wind-driven currents prevail over tidal or density-driven currents due to the narrow shelves and the relatively low river discharges (González et al., 2004; OSPAR, 2000). The interaction of the IPC with the abrupt bathymetry often generates eddies (e.g. Pingree and Le Cann, 1992a; Rubio et al., 2018). Transport and retention conditions at the surface vary at interannual, seasonal and even daily scales, influenced by the general circulation and various coastal processes such as wind-driven currents and mesoscale structures (Rubio et al., 2020).

The main aim of this work is to provide further insight into the effect of circulation on the distribution of ELS anchovies. To this end, Lagrangian diagnostics were performed, primarily focusing on computing transports. Transports were computed considering three key factors:

(i) *The use of multiplatform observations*. The initial distributions were set from the observed abundances from BIOMAN surveys and transport computations relied on currents observed by a high-frequency radar (HFR) system. HFRs provide reliable surface velocity measurements worldwide (Reyes et al., 2022; Roarty et al., 2019; Rubio et al., 2017) and are used to validate models (see references in De Mey-Frémaux et al., 2019). The HFR system used in this study belongs to the Basque Operational Oceanography System (EuskOOS, https://www.euskoos.eus/en/;Fig. 1b), which has widely demonstrated its ability to accurately represent the circulation in the study area (Rubio et al., 2011, 2013, 2018, 2020; Solabarrieta et al., 2014, 2015, 2016) and to perform

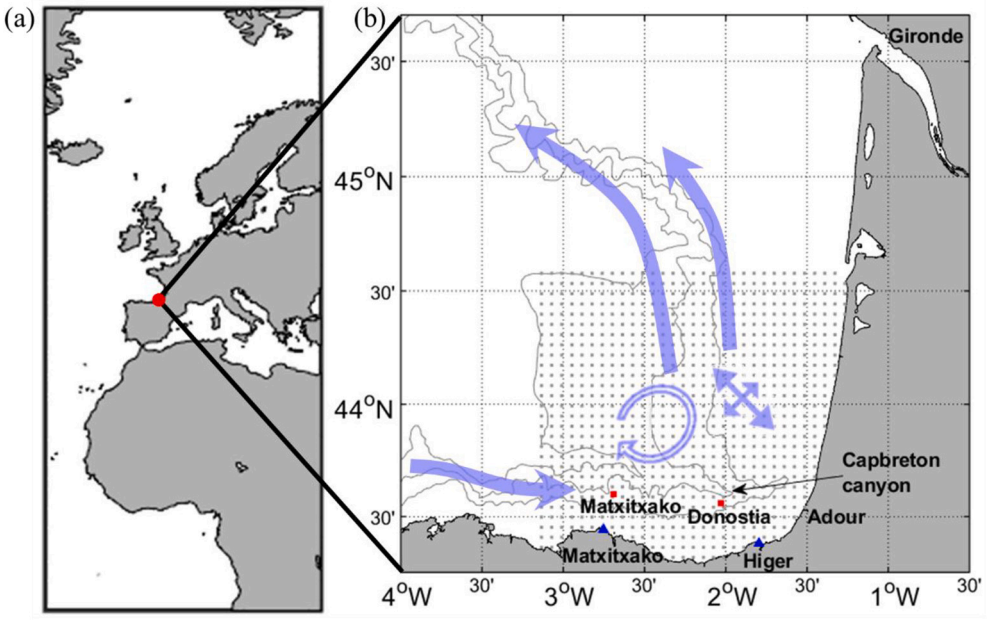

Fig. 1. (a) Location of the study area depicted by the red dot. (b) Location of the EuskOOS HFR antennas (blue triangles), HFR grid points (grey points) and ADCP moorings (red squares). Capbreton canyon and Gironde and Adour rivers mouths are also depicted. Blue light symbols show the main circulation drivers: the winter IPC (big solid arrows), mesoscale eddies (hollow circular arrow, note that eddies can be cyclonic or anticyclonic) and wind-driven currents (double solid arrow). Grey lines show the 200, 1000 and 2000 m isobaths. (For interpretation of the references to colour in this figure legend, the reader is referred to the web version of this article.)

accurate surface Lagrangian diagnostics (Hernández-Carrasco et al., 2018b; Rubio et al., 2013; Solabarrieta et al., 2016).

(ii) *The use of a carefully selected integration period.* Transport computations were performed for an integration period where ELS anchovies could be considered passive particles. The development of the swimming abilities and their susceptibility to currents depend on their size, which in turn is influenced by environmental factors like temperature. Based on the work of Cotano et al. (2008) and Aldanondo et al. (2008, 2010) active movements can be deduced for approximately 20–22 days (or longer) after hatching, although this does not imply that anchovies are not still transported. Irigoien et al. (2008) mention that they actively swim 30–40 days after hatching when they metamorphose into juveniles. Therefore, a 30-day integration period was chosen.

(iii) *Surface and subsurface levels*. The characterization of the net vertical transport of ELS anchovies is complex. Buoyancy or diel vertical migration (DVM)-driven movements can affect transport, however, they are roughly parametrized in transport studies (e.g. Edwards et al., 2007; Huret et al., 2010; Ospina-Alvarez et al., 2012; Palatella et al., 2014; Parada et al., 2008). Besides, the existing models barely solve vertical currents in the area. Based on vertical distribution and velocity information, surface and subsurface levels were set for horizontal transport computations. Eggs are more abundant within the first 20 m with mean depths ranging from 3 to 8 m (Boyra et al., 2003; Coombs et al., 2004). At larvae stages, not much is known about vertical distribution and therefore DVM. Hence, observations of European anchovy larvae in the Mediterranean Sea were considered, which showed the highest average abundances in the upper 20 m and particularly close to the surface (Olivar et al., 2001; Palomera, 1991). Given the vertical currents lower than 1 m day^{-1} observed inside an eddy (where vertical movements are stronger than average except for intense frontal areas (e.g. Capó et al., 2021; Tarry et al., 2022)) in the study area (Caballero et al., 2016), computations at 3 (surface level) and 10 m (subsurface level) were considered. Surface computations utilized HFR data, while velocities for the subsurface ones were obtained by reconstructing HFR and acoustic Doppler current profiler (ADCP) data by a reduced order optimal interpolation (ROOI) method. Despite also using model data, this method strongly constrains the reconstructions to the observations and has been successfully tested in the area (Manso-Narvarte et al., 2020, 2021).

Despite the assumptions made and limitations of the used approach, this study provides a novel insight into the effects of circulation on ELS anchovies' distribution. Transport patterns were analysed by a multi-year analysis and from a process-oriented perspective supported by additional advanced Lagrangian diagnostics such as Lagrangian Coherent Structures (LCS). The results showed high variability across different computation periods while revealing common patterns, such as retention in the slope and shelf areas. Additionally, various coastal processes were identified as factors that might influence ELS anchovies' distribution and circulation could increase aggregation at short time scales (20 days).

2. Data

In the following subsections, the datasets used are described as summarized in Fig. 2.

2.1. Observational velocity data

Observational velocities were provided by the EuskOOS HFR system and the ADCPs located in two slope moorings. The HFR system consists of two sites located at Cape Higher and Cape Matxitxako (Fig. 1b). It

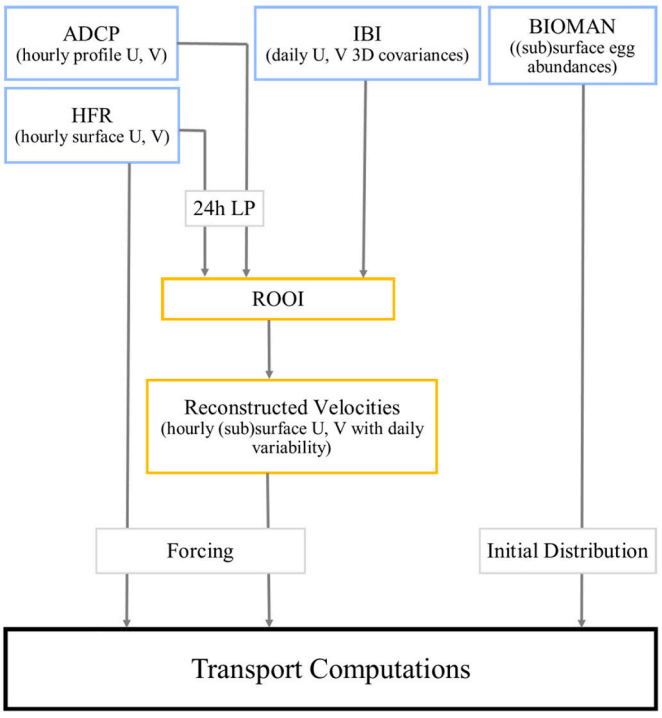

Fig. 2. Summary of the observing platforms and datasets used for the transport computations and the ROOI method. LP means low-pass filtered and U and V are the zonal and meridional components of the currents, respectively.

works at a central frequency of 4.46 MHz, with an operational bandwidth of 30 kHz, providing hourly surface velocity fields gridded in a regular mesh of 5 km resolution. It covers ~150 km off the coast and represents the first ~1.5 m of the water column. This system has been providing surface currents since 2009 (Rubio et al., 2011, 2013, 2018, 2020; Solabarrieta et al., 2014, 2015, 2016) with some interruptions mostly due to severe atmospheric conditions. Two downward-looking ADCPs (located at the Donostia and Matxitxako moorings; Fig. 1b) working at a central frequency of 150 kHz provided time series of hourly velocities from 12.26 m to 200 m in the water column with bins every 8 m since 2007 (Rubio et al., 2013; Solabarrieta et al., 2014).

HFR and Donostia ADCP velocities were used as input observations for the ROOI method. Additionally, HFR velocities were used as forcing data in surface computations and the estimation of LCSs. Matxitxako ADCP velocities were used in the sensitivity tests to select the optimal parameters for applying the ROOI method, shown in *Supplementary Data* (*SD*) *1*. Furthermore, they were used in the ROOI validation exercises in *SD 2*.

HFR velocities were spatially gap-filled to ensure the spatiotemporal continuity in the velocity fields needed to perform accurate Lagrangian diagnostics. The data-gap filling was carried out by the open-mode analysis (OMA) method (Kaplan and Lekien, 2007), which provides reliable velocities for these diagnostics (Hernández-Carrasco et al., 2018b). HFR velocities were quality-controlled using procedures based on velocity and variance thresholds, signal-to-noise ratios, and radial total coverage, following standard recommendations (Mantovani et al., 2020). ADCP velocities were quality-controlled by beam amplitude and correlation magnitudes and velocity errors following Bender and DiMarco (2009).

2.2. Reanalysis model velocity data

The IBI_REANALYSIS_PHYS_005_002 data product (hereinafter IBI) provided by Copernicus Marine Environment Monitoring Service (CMEMS) was used as velocity data input to compute the covariance

matrix for the ROOI method. Additionally, this dataset was used in the ROOI validation exercises shown in *SD 2*. IBI is based on a realistic configuration of the NEMO model for the Iberian Biscay Irish region and assimilates in-situ and satellite data. For more information, the reader is referred to Sotillo et al. (2015).

IBI provides daily data with unevenly distributed vertical levels with separations between 1 and 3 m in shallow depths and increasing separations with depth. The horizontal resolution is of 0.083° x 0.083° (~6–9 km).

2.3. Anchovy egg distribution data

The initial particle distributions used in the transport computations were based on the anchovy egg abundances observed during the BIOMAN surveys, run in the BoB every year around May (Santos et al., 2011; doi:10.57762/N22G-WQ88). Egg abundance samples were collected along 15 nautical miles (nmi)-separated transects (7.5 nmi in areas of high abundance) perpendicular to the coast (see Fig. 3) by means of two systems. On the one hand, the Continuous Underway Fish Egg Sampler (CUFES; Checkley et al., 1997) pumped water at 3 m onboard and recorded the eggs with a net of 335 μm mesh size. Then, samples were immediately checked providing real-time abundances every 1.5 nmi. On the other hand, vertical hauls were made every 3 nmi along the survey transects using a PairoVET net (i.e. 2-CalVET nets; Smith et al., 1985) with a 150 μm mesh. After lowering the net down to 100 m, it was lifted back and anchovy eggs were fixed in formaldehyde 4% buffered with sodium tetra borate in seawater. Then they were sorted, identified (according to Moser and Ahlstrom (1985)) and counted onboard. CUFES represents the egg abundance at 3 m, whereas PairoVET integrates the upper 100 m of the water column. Given that eggs are mainly located in the upper 20 m (Boyra et al., 2003; Coombs et al., 2004), PairoVET samples are allocated at 10 m.

2.4. Wind and chlorophyll-a data

Wind data and chlorophyll-a (Chl-a) images were used to complement the process-oriented analyses. Hourly wind data were extracted at 43.86°N–2.14°W from the Weather Research and Forecasting model (WRF) of the meteorological agency of Galicia (MeteoGalicia). This model is able to reproduce the wind fields of the SE-BoB with reasonable accuracy (Ferrer et al., 2010). On the other hand, daily level 3 Chl-a images (for dates sufficiently free of clouds) with a 1 km resolution were obtained from the OCEANCOLOUR_ATL_CHL_L3_REP_OBSERVATIONS_009_067 data product of CMEMS.

3. Methods

In this section, the implementation of the ROOI method is first presented, followed by the transport computations set-up, and finally, the metrics used to analyse the outcomes of the computations.

3.1. Reduced Order Optimal Interpolation (ROOI) reconstructions

The ROOI method, first used by Kaplan et al. (1997), is based on Empirical Orthogonal Function (EOF) decomposition. It uses historical information to compute spatial covariances between the observation points and the points where observations are going to be extended. Then an EOF decomposition is applied to the covariance matrix and only the leading modes are kept (accounting for the biggest part of the variability), thus ignoring higher-order modes that could introduce noise in the reconstructions. The reconstructed fields are obtained by extending the available observations to all the grid points based on those modes and by minimising the deviation between the reconstructions and observations. For a more complete description of the method see Kaplan et al. (1997), Jordà et al. (2016) or Manso-Narvarte et al. (2021). The ROOI method has been already used in the study area to reconstruct

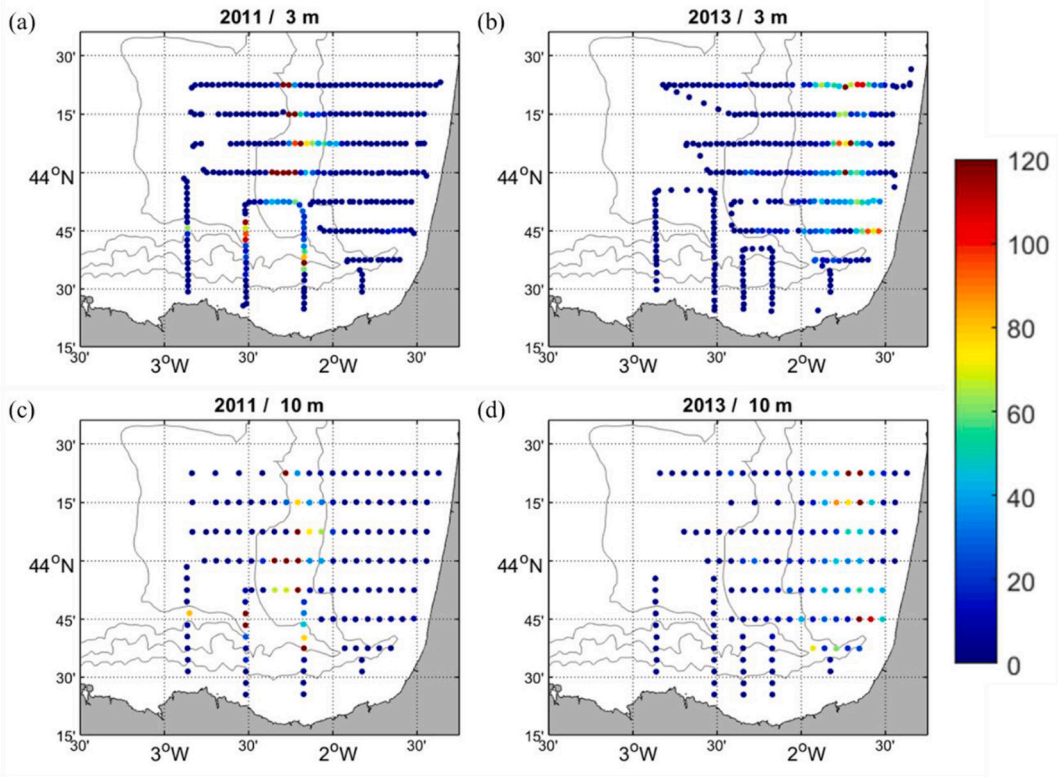

Fig. 3. Distribution of the 10,000 particles according to observations of the CUFES system at 3 (a, b) and of the PairoVET system at 10 m (c, d). (a) and (c) correspond to the period centred on 10 May 2011, whereas (b) and (d) correspond to the period centred on 13 May 2013. The colorbar depicts the number of particles and the grey lines show the 200, 1000 and 2000 m isobaths.

subsurface velocities from multiplatform observations obtaining mean spatial errors between 0.55 and 7 cm s^{-1} and mean relative errors of 0.07–1.2 times the root mean square value for the first 150 m (Manso-Narvarte et al., 2020, 2021).

Velocities were reconstructed at 3 and 10 m (hereinafter ROOI velocities) from the HFR and Donostia ADCP observations and the covariance matrix extracted from IBI (as indicated in Fig. 2). HFR and ADCP hourly velocities were 24 h low-pass filtered to match the covariances' daily variability, thus providing hourly ROOI velocities, with a daily variability at the same spatial resolution as IBI. For all the reconstructions, the number of modes selected was 100 and the observational error of the velocities was 2 cm s^{-1}. This configuration led to reasonable results in Manso-Narvarte et al. (2021) and in the comparisons with Matxitxako ADCP velocities (see *SD 1*).

3.2. Transport computations set-up

To compute the transport of ELS anchovies as infinitesimal passive particles, the Lagrangian module of the MOHID Water software (Leitão, 1996; Neves, 2013) was used. The computation grid was set to 2.25 × 3.1 km with a slip boundary condition at the South and East sides of the domain (coastal areas) to avoid the removal of particles. The slip condition was set due to the scarce resolution nor coverage of observational currents in the coastal area to properly parametrize the complex beaching processes. At the North and West areas (open boundaries) particles were allowed to leave the domain. The module uses an Euler scheme with a time step of 15 min to integrate the equation of motion, and a bilinear interpolation in space and linear interpolation in time of the velocity fields at the particle positions. The equation of motion includes a diffusion term with a diffusivity value of 4 m^2 s^{-1}, based on Okubo (1971).

Transport computations were performed for seven periods corresponding to the yearly BIOMAN surveys from 2011 to 2018, excluding 2015 due to the lack of available velocity data. The data used and the scheme followed in the transport computations are summarized in Fig. 2. In each period 10,000 particles were initially distributed according to the observations from CUFES at 3 m and PairoVET at 10 m, for surface and subsurface computations, respectively. An example of the initial particle distributions for 2011 and 2013 is shown in Fig. 3. The starting dates were determined as the mean date of the BIOMAN survey in the study area (which represents a period of 3 days where the abundance distributions are stable): 10 May 2011; 13 May 2012; 13 May 2013; 8 May 2014; 9 May 2016; 9 May 2017 and 13 May 2018. Transports were computed for an integration period of 30 days, as explained in the Introduction.

The ROOI velocities demonstrated to fairly reproduce currents at 10 m (see *SD 2*), however, their availability depends on the simultaneous availability of HFR and ADCP velocities. On the other hand, high temporal continuity in the velocity fields is needed to perform accurate transport computations. Consequently, surface and subsurface computations forced by ROOI velocities were only performed for 2011 and 2013. Surface computations forced by HFR velocities were performed for all the above-mentioned years, thus providing a wider time coverage.

3.3. Metrics

Metrics used to analyse the outcomes of the transport computations were particle distributions, their centre of mass (CM) and LCS obtained from Finite Size Lyapunov Exponents (FSLE).

3.3.1. Particle distributions and centre of mass (CM)

Particle distributions are depicted by the number of particles per computation grid cell, whereas the CMs provide the position of their centres. The position of the latitude and longitude of the CM were estimated separately as follows:

$$CM_{longitude} = \frac{\sum_i n_i \cdot longitude_i}{N} \quad (1)$$

$$CM_{latitude} = \frac{\sum_i n_i \cdot latitude_i}{N} \quad (2)$$

where i is the position of the grid cell, n_i the number of particles in the i-th cell, $longitude_i$ and $latitude_i$ the position in the i-th cell and N the total number of particles. CMs at different days of the transport computations were used as a proxy for the overall transport of particles.

3.3.2. Finite Size Lyapunov Exponents (FSLE)

One of the most widely used Lagrangian diagnostics to study coastal transport is the so-called LCS, which are roughly defined as material lines that act as transport barriers such as eddy boundaries or fronts (Haller, 2015; Haller and Yuan, 2000; Hernández-Carrasco and Orfila, 2018; Shadden et al., 2009). Since particles cannot cross them, LCS determine the flow motion, providing a template of the flow geometry. One of the standard approaches for obtaining LCS is to compute FSLE (Boffetta et al., 2000). In a 2D flow the value (denoted by λ) at the position (x,y) and time t, is obtained by measuring the minimum time T, taken for two neighbour trajectories, initially separated by a finite distance δ_0, to reach a larger final finite distance δ_f, using the following formula:

$$\lambda(x,y,t) = \frac{1}{T} ln \frac{\delta_f}{\delta_0} \quad (3)$$

FSLE provide temporal and spatial scales for the dispersion and stirring processes of fluid parcels and the largest values indicate LCS (d'Ovidio et al., 2004; Hernández-Carrasco et al., 2011). High FSLE estimated forward in time depict a high rate of trajectories' separation and therefore repelling LCS. Conversely, high values of FSLE estimated backwards in time indicate a high rate of trajectories' convergence and therefore attracting LCS.

LCS computed from HFR velocities have been already used to study the role of coastal transport on phytoplankton distribution (Hernández-Carrasco et al., 2018a; Rubio et al., 2018). In this study, FSLE estimated backwards in time were used to identify coastal processes that affect transport patterns. FSLE were obtained following the algorithm described in Hernández-Carrasco et al. (2011). The integration of the particle trajectories was carried out using a 4th order Runge-Kutta scheme with a time step of 15 min, and the velocity fields at the particle positions were interpolated bilinearly in space and linearly in time. Particles were advected during a total integration time of 15 days.

4. Results

In this section, first, the multiyear variability of transport patterns is analysed at the surface, and then the differences between surface and subsurface levels. These results are shown by the position of the CMs at 3, 10, 20 and 30 days of the transport computations, while snapshots of particle distributions are presented in *SD 3* to support the description of the results. Finally, coastal processes affecting transport patterns are analysed by comparing particle distributions with LCS, Chl-a images and wind data.

4.1. Multiyear analysis of surface transport patterns

Surface computations forced by HFR velocities were used to analyse the multiyear variability of transport patterns. Snapshots of the initial particle distributions for the whole set of analysed years are provided in *Figs. SD4* and *SD5*. The initial conditions varied: in 2012, 2013, 2014, 2016, 2017 and 2018 particles were distributed over the French shelf, while in 2011, 2017 and 2018 particles were additionally found over the slope and even off the shelf in 2017.

In 2011, particles first travelled southwestwards with almost 30% of them leaving the domain through the southwestern boundary. Then, they were transported southeastwards during the last 10 days (Figs. 4b and *SD4a-e*). In 2012, particles remained mainly over the French shelf without travelling long distances (Figs. 4b and *SD4f-j*) and with only 2% of them leaving the domain. In 2016, they also remained over the French shelf, being slightly transported southwards and 14% of particles left the domain (Figs. 4c and *SD5a-e*). In 2013, particles remained over the French shelf during the first 20 days and then travelled northwestward for the last 10 days (Figs. 4b and *SD4k-o*). Around 18% of particles left the domain through the northern boundary. In 2014, most of the particles were initially distributed over the French shelf and the CMs remained there for 30 days (Fig. 4c) with some particles distributed around the shelf-break and slope area and the rest in the inner part of the shelf (*Fig. SD4p-t*). Only 10% of particles left the domain. In 2017, 35% of particles left the domain through the northern boundary after the third day, changing the position of the CM to the south (Fig. 4c). The rest of the particles moved slightly southwards but remained around their initial position over the shelf and slope (see *Fig. SD5f-j*). In 2018, particles initially distributed over the Spanish slope were transported eastwards, whereas the ones over the French shelf, which composed the bulk of the particles, were transported southwestwards (Figs. 4c and *SD5k-o*). Particles initially distributed at the northern part of the domain over the French shelf were transported off-shelf, with 24% of them leaving the domain through the northwestern boundary.

4.2. *Differences between surface and subsurface transport patterns*

For comparing surface and subsurface transport patterns, computations forced by ROOI velocities for 2011 and 2013 were used. The initial particle distributions in 2011 and 2013 were similar at both levels, with particles mainly located over the French slope and shelf, respectively (see *Fig. SD6* for the initial particle distribution snapshots). In 2011, a significant number of particles (35% and 40% at surface and subsurface levels, respectively) left the domain mostly through the northwestern boundary before they travelled southeastwards. Conversely, in 2013 most of the particles remained in the domain with domain-leaving rates of 10 and 0% at surface and subsurface levels, respectively.

In 2011, the CMs' trajectories at both levels differed after 3 days

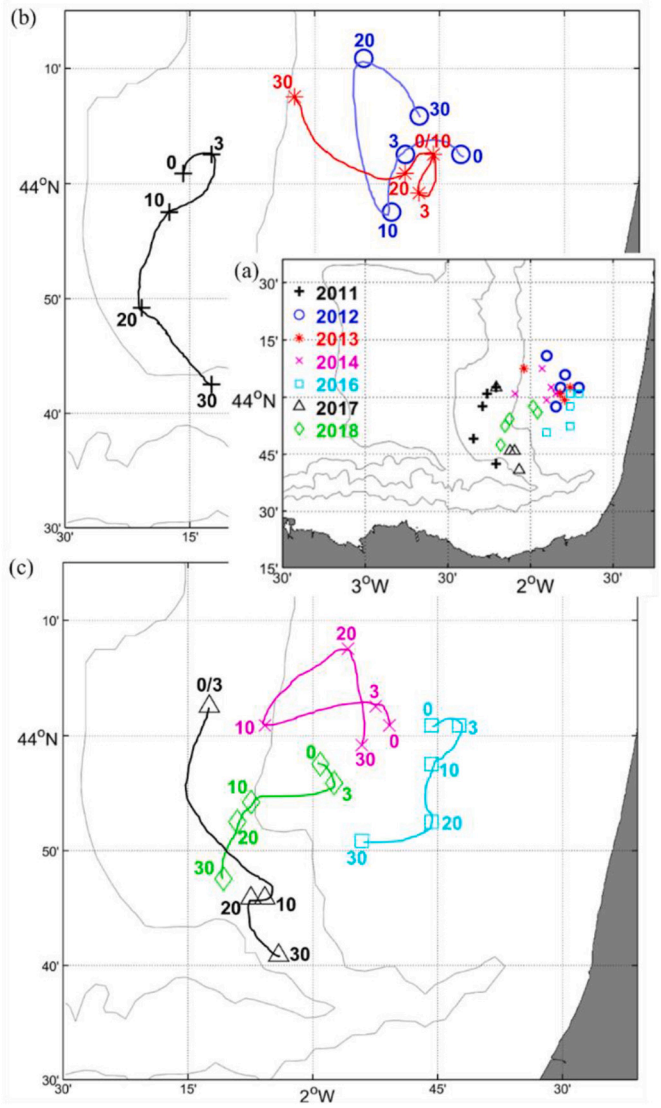

Fig. 4. (a) Position of the CMs at surface level (3 m) for different years, corresponding to transport computations forced by HFR velocities. (b) zoomed for 2011, 2012 and 2013. (c) zoomed for 2014, 2016, 2017 and 2018. The numbers 0, 3, 10, 20 and 30 mean the days of computation. The lines show the trajectory of the CMs. The grey lines show the 200, 1000 and 2000 m isobaths.

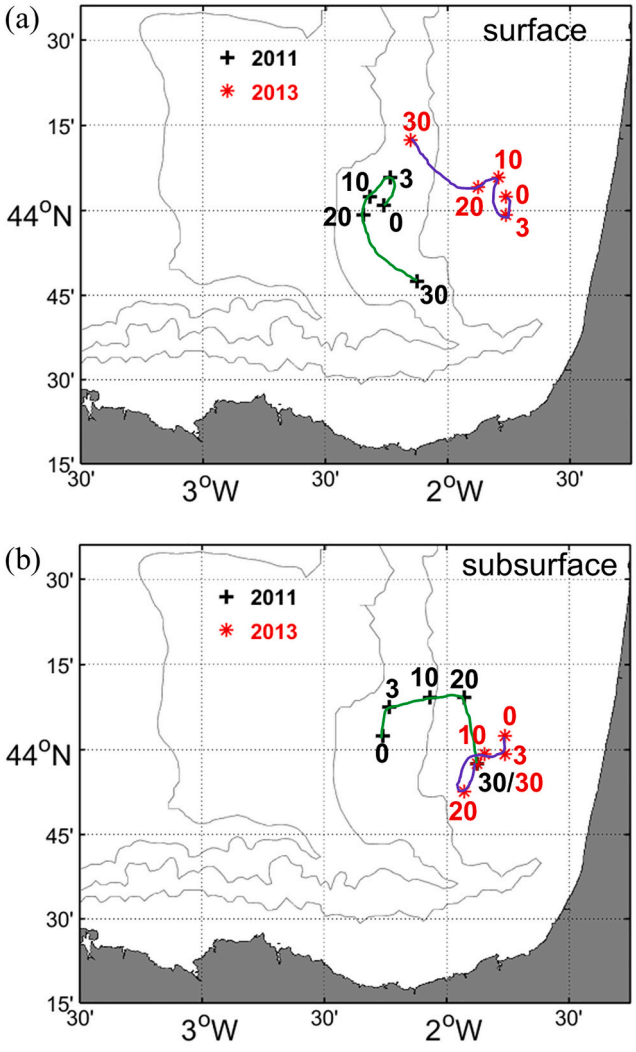

Fig. 5. Position of the CMs at (a) surface (3 m) and (b) subsurface (10 m) levels for 2011 (black crosses) and 2013 (red asterisks). The numbers 0, 3, 10, 20 and 30 mean the number of computation days. The green and purple lines show the trajectory of the CMs in 2011 and 2013, respectively. The grey lines show the 200, 1000 and 2000 m isobaths. (For interpretation of the references to colour in this figure legend, the reader is referred to the web version of this article.)

(Fig. 5), although the particle distributions had a similar shape (*Fig. SD6a-j*). However, in the last 10 days, they again showed a similar displacement. In 2013, particles mainly remained over the French shelf at both levels (Figs. 5 and *SD6k-t*) showing similar transport patterns during the first 20 days. In the last 10 days, transport patterns differed. For both analysed years and levels, the CMs remained over the French shelf and slope.

4.3. Coastal processes affecting transport patterns

Surface computations forced by HFR velocities were used to analyse the impact of coastal processes on transport patterns. Various mesoscale structures were identified, namely, eddies, fronts and along-slope currents within the slope and Capbreton canyon. In some periods, particles were also affected by spatially homogeneous wind-induced currents. In Figs. 6–9, these processes are represented by examples of specific periods.

An eddy case is displayed in Fig. 6 where a high number of particles was distributed around an anticyclonic eddy centred at 43.9°N-2.25 W° in 2011. The eddy was identified both by LCS and Chl-a images. This situation persisted for around a week (not shown). Another example is shown in *Fig. SD7* in 2016 where particles were trapped around an eddy located at the head of the Capbreton canyon. Note that areas with a high number of particles correspond to areas of high FSLE values that represent attracting LCS.

A front case is shown in Fig. 7 where an intense Chl-a gradient was observed over the French shelf and shelf-break area (e and f panels, respectively) in 2013. High Chl-a waters were concentrated around the areas constrained by LCS and the front seemed to act as a transport barrier blocking the motion of particles towards the open ocean. The effects of fronts were also observed in other periods: in 2012 particles were aggregated along a frontal area and then moved northwards along with the movement of the front (*Fig. SD 8*), while in 2016 a frontal area along the French coast blocked the movement of the particles towards the open ocean (*Fig. SD 7*).

A case where the transport of particles was constrained by along-slope currents within the slope and Capbreton canyon is depicted in Fig. 8 where particle distributions and LCS show this situation for one week in 2011. In 2017, despite having weak along-slope currents, particles were trapped at the head of the Capbreton canyon and slope areas for around two weeks (*Fig. SD9*).

A case where the transport of particles was not linked to any mesoscale structure is represented in Fig. 9 in 2014. Strong southern winds (Fig. 9g) drove surface currents from 21 to 26 May inducing a northward transport (Fig. 9a-d) and particles were slightly aggregated towards the French coast, likely due to rightward deflection by the Ekman currents. This was also noticeable in the Chl-a images in the northeastern area (Fig. 9ef). Note that some particles were retained around the Spanish slope area on 18 May (Fig. 9a) where a front is observed both by a Chl-a image (Fig. 9e) and LCS (Fig. 9c).

Despite the identification of different coastal processes, the resulting transport patterns are most likely due to a combination of them. In 2011 an eddy influenced the transport of particles (Fig. 6) and after strong southward winds (not shown), the eddy disappeared, and particles were trapped and transported along the slope and Capbreton canyon area (Fig. 8). In 2016 an eddy located at the head of the Capbreton canyon and a front along the French coast constrained the transport of particles simultaneously (*Fig. SD 7*).

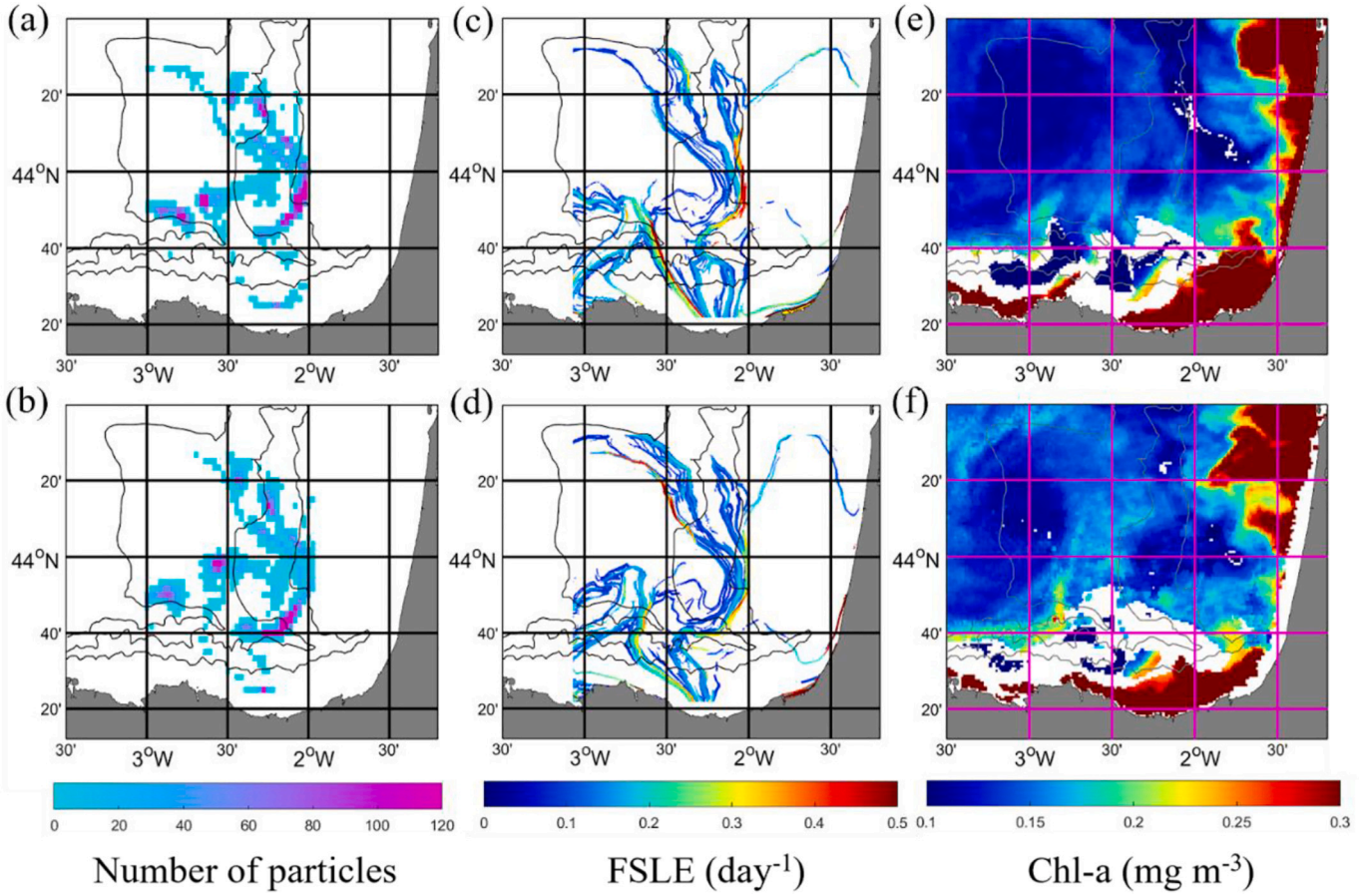

Fig. 6. (a, b) Particle distributions (number of particles per computation grid cell), (c, d) FSLE (day^{-1}) and (e, f) Chl-a concentrations (mg m^{-3}) in 2011 for 25 May (a, c, e) and 28 May (b, d, f) showing the eddy case. The grey lines are the 200, 1000 and 2000 m isobaths.

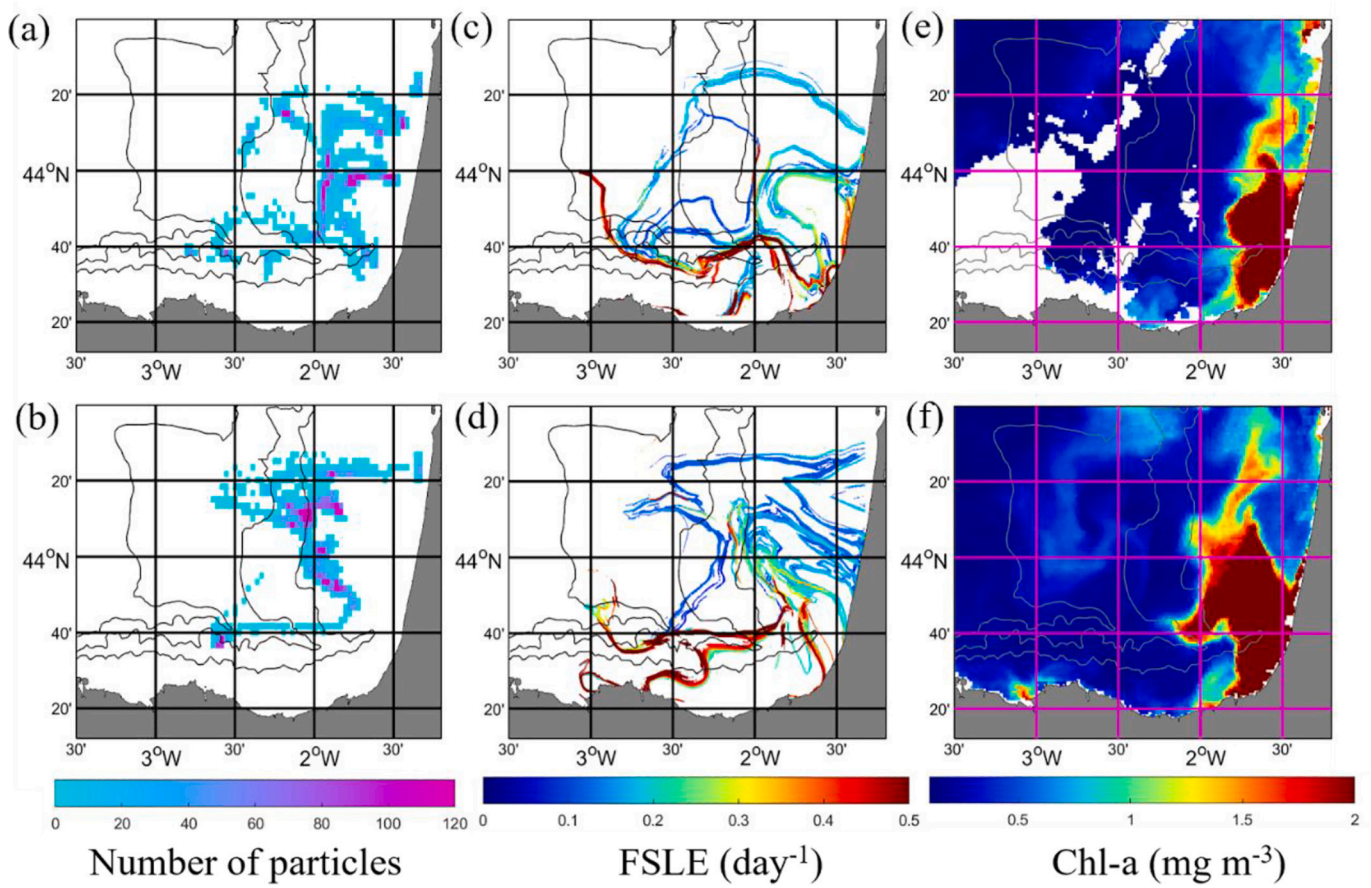

Fig. 7. (a, b) Particle distributions (number of particles per computation grid cell), (c, d) FSLE (day^{-1}) and (e, f) Chl-a concentrations (mg m^{-3}) in 2013 for 26 May (a, c, e) and 5 June (b, d, f) showing the front case. The grey lines are the 200, 1000 and 2000 m isobaths.

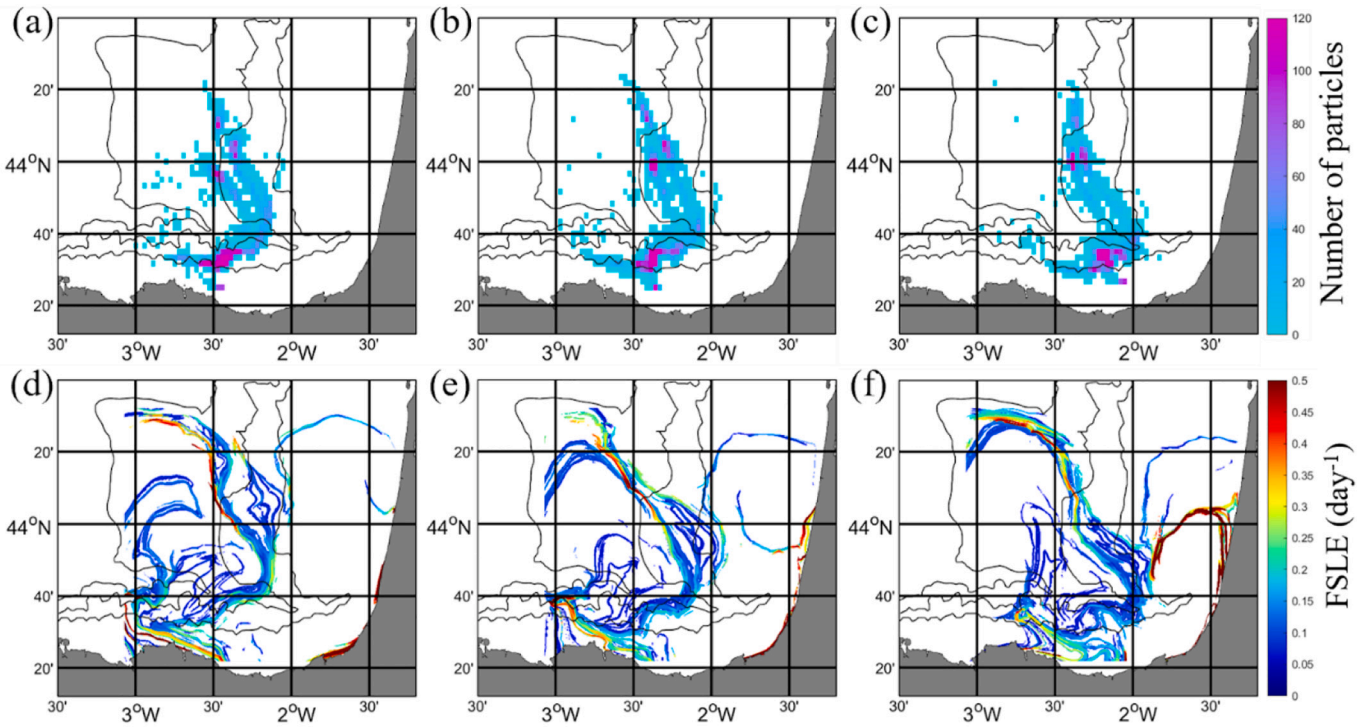

Fig. 8. (a, b, c) Particle distributions (number of particles per computation grid cell), and (d, e, f) FSLE (day^{-1}) in 2011 for 1 (a, d), 5 (b, e) and 8 (c, f) June showing the case where particles are affected by the along-slope current regime within the slope and Capbreton canyon areas. The grey lines are the 200, 1000 and 2000 m isobaths.

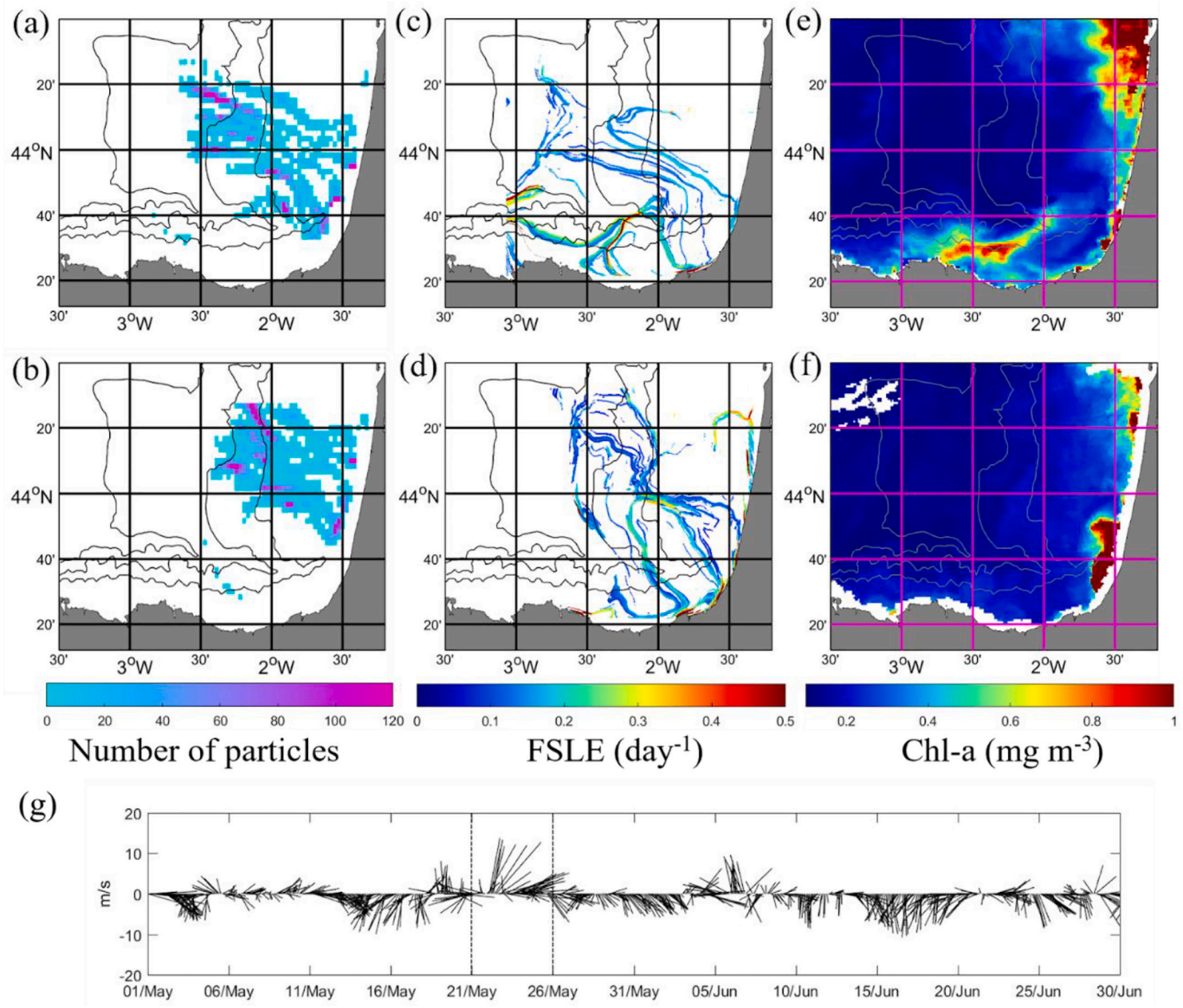

Fig. 9. (a, b) Particle distributions (number of particles per computation grid cell), (c, d) FSLE (day^{-1}) and (e, f) Chl-a concentrations (mg m^{-3}) in 2014 for 18 May (a, c) and 27 May (b, d) showing the case where there is not any mesoscale structure and particles are affected by the wind. (g) Wind series at 43.86°N-2.14°W where a strong wind period is delimited by the black dashed lines between 21 and 26 May. The grey lines are the 200, 1000 and 2000 m isobaths.

5. Discussion

A new approach for analysing how circulation influences the distribution of ELS anchovies was employed. For the first time in the area, their transport was analysed purely based on observations and for periods where their passive behaviour could be assumed based on previous works. Transport computations show how circulation induces aggregation regardless of the initial particle distributions (see *Figs. SD4–6*). The high variability of surface transport patterns (Fig. 4), induced by the different spatiotemporal scales of circulation, was also observed in the study area in previous ELS anchovy transport computations (Allain et al., 2001, 2007; Ferrer et al., 2004; Huret et al., 2010) or for passive tracers in general (Rubio et al., 2020). This variability was much higher than that related to seasonal wind patterns (Cotano et al., 2008; Irigoien et al., 2008; Uriarte et al., 2001). Higher coastal retention was observed when particles were initially distributed over the shelf, stressing that the spawning location likely affects the subsequent retention. Moreover, the CMs did not get further west than the French slope (off the French coast) and particle domain-leaving rates ranged from 0 to 35%, indicating that ELS anchovies do not tend to disperse towards the open ocean. This pattern agrees with the one computed by Ferrer et al. (2004) and differs from the ones computed by Allain et al. (2001, 2007) and Huret et al. (2010) who, in general, suggested stronger offshore transport in the study area. This disparity might be attributed to the different periods and assumptions (e.g. initial distributions, forcings, integration times) considered. Differences in the ocean processes solved may also lead to discrepancies. Huret et al. (2010) mention that the complex processes around the shelf-break area, such as the intrusion of the IPC or the slope instabilities, might be weakly resolved in their model, while Allain et al. (2001) acknowledge that the local retention mechanisms near the coast may be underestimated by theirs. These processes have been specifically analysed with the HFR and ADCP data (Rubio et al., 2018, 2019; Solabarrieta et al., 2014), highlighting the benefit of using observed currents to study transports and stressing the potential of coastal observatories for integrated studies. In addition, the potential of observations to improve models by validation or assimilation procedures is also emphasized.

Surface and subsurface computations partially agreed (Figs. 5 and

SD6). Discrepancies could be caused by the differences in the initial particle distributions and circulation between both levels. May is a transition period from mixed to stratified conditions in the study area (Rubio et al., 2013), thus, current shear will vary depending on the year with its subsequent effect on transport patterns. Consequently, transport computations at each depth are relevant. However, in the absence of subsurface computations, surface computations, which provide a wider time coverage, can partially represent what happens in the subsurface.

Eddies, fronts and along-slope currents within the slope and Capbreton canyon areas were identified as mesoscale structures that can shape the distribution of ELS anchovies (Figs. 6–9). In some periods, a combination of these processes along with the effect of the wind resulted in complex transport patterns. These results are in agreement with previous studies which observed that wind-driven currents and mesoscale structures affect surface water transport patterns in the study area (Rubio et al., 2018, 2020; Ruiz et al., 2020). Particularly, Rubio et al. (2018) reported that eddies regulate cross-shelf coastal water exchanges at the surface. Besides, slope eddies were already suggested to be responsible for the retention of ELS anchovies by transporting them off the shelf, while limiting their dispersion towards the open ocean (Irigoien et al., 2008). Although these eddies usually travel westward, they can remain in the area (Caballero et al., 2008, 2014; Garcia-Soto et al., 2002; Pingree and Le Cann, 1992a, 1992b) for enough time to keep the larvae near the shelf-break until they develop swimming abilities and move back to the shelf. Eddies have been also identified as fish larvae retention mechanisms in other geographical areas (e.g. Mullaney and Suthers, 2013; Rodríguez et al., 2004; Sabatés et al., 2007a; Somarakis and Nikolioudakis, 2007). The effect of fronts in shaping transport and connectivity patterns is a ubiquitous feature within the ocean present at different spatiotemporal scales (e.g. Garden et al., 2014; Hernández-Carrasco and Orfila, 2018; Lehahn et al., 2007). In the study area, small fronts were identified as structures aggregating floating marine litter (Ruiz et al., 2020) and as transport barriers between coastal and offshore waters. The transport constraint by along-slope currents in the study area was also already detected by Rubio et al. (2018) who observed weak surface water exchange across the shelf-break and intense transport through the northern limit under typical northward IPC conditions. A similar pattern was observed in the NW Mediterranean, where the Northern Current limited the dispersion of fish larvae towards the open ocean (Sabatés et al., 2007a) and also transported them along the slope (Sabatés et al., 2007b). The retention within the slope and Capbreton canyon in periods of low-intensity slope currents (*Fig. SD9*) might be triggered by unknown current-topography interactions that deserve a specific investigation due to their potential impact on biological and environmental processes.

Even with certain limitations, such as the lack of enough reconstructed velocities to sufficiently cover some integration periods, the utility of the ROOI method to exploit multiplatform observations and for coastal transport Lagrangian studies has been showcased. Reconstructed subsurface velocities could help to better understand transport patterns in the water column, complementing the analysis made at the surface by Rubio et al. (2018, 2020). Subsurface currents could be also used to study the retention conditions within the slope and Capbreton canyon.

Although the proposed approach presents various limitations, it still enables significant analyses and opens up future work:

- The spatial extension of the study area was limited by the HFR coverage and the diagnostics were only performed when BIOMAN data were available in May. Even though, the results cover one of the main anchovy spawning areas at peak spawning periods (Motos et al., 1996). Lagrangian diagnostics at the basin scale from BIOMAN egg abundances and accurate model or reanalysis currents would broaden the present work.
- During the last 10 days of the integration period, a fraction of the ELS anchovies might exhibit mobility. Nevertheless, their movement is weak and they are still notably affected by currents, thus not influencing the results. In fact, even if only 20 days of integration are considered the results lead to the same conclusions.
- As explained in the Introduction, the vertical transport by currents, buoyancy or DVM was not considered. For including vertical movements in future studies further characterization of the DVM would be necessary in the study area, as well as a model-based approach to perform 3D Lagrangian diagnostics. Yet, the observation-based findings of the present study could aid the interpretation of those analyses.
- This study focuses on the effect of circulation on ELS anchovies' distribution, however, the biological implications of the results should be investigated in the future. Field samples collected by ad-hoc oceanographic surveys 30 days after BIOMAN can contribute to achieving this goal. Additionally, these surveys would aid in testing the impact of the assumptions of the present approach.

All in all, the used approach offers an invaluable framework to address biophysical interactions and can be also applied to other species, other kinds of passive particles or other areas.

6. Summary and conclusions

The effects of circulation on ELS anchovies' distribution were analysed considering ELS anchovies as passive particles in the peak spawning period in the SE-BoB. To that end, surface and subsurface Lagrangian diagnostics were performed using observed and reconstructed horizontal velocities and with the initial particle distributions set from in-situ observations over several years. Transport patterns were highly influenced by the different spatiotemporal scales of circulation, and overall, the results suggest that ELS anchovies are retained in the study area with lower retention for eggs spawned over off-shelf areas. Together with wind-induced currents, eddies, fronts and along-slope currents within the slope and the Capbreton canyon area were suggested as ocean processes strongly affecting the distribution of ELS anchovies. The results also suggest that circulation can play a key role in ELS anchovy aggregation within short time scales (20 days).

In the future, the present study should be extended to the whole BoB and vertical transport should be considered. The biological implications of the present findings should be also analysed. Additionally, the use of reconstructed currents from multiplatform observations would enable to analyse transport patterns in the water column, for a better understanding of interactions between physical and environmental or biological processes. This study highlights the potential of observation-based approaches and coastal observatories for conducting integrated investigations.

Declaration of Competing Interest

The authors declare that they have no known competing financial interests or personal relationships that could have appeared to influence the work reported in this paper.

Data availability

The datasets used in this study are available at the following links:

- HFR: https://www.euskoos.eus/en/data/basque-ocean-meteorological-network/high-frequency-coastal-radars/
- ADCP:https://www.euskoos.eus/en/data/basque-ocean-meteorological-network/donostia-deep-water-buoy/
- IBI:https://resources.marine.copernicus.eu/?option=com_csw&view=details&product_id=IBI_MULTIYEAR_PHY_005_002
- BIOMAN: Data can be available on request: doi:10.57762/N22G-WQ88
- Chl-a images:https://resources.marine.copernicus.eu/?option=com_csw&view=details&product_id=OCEANCOLOUR_ATL_CHL_L3_REP_OBSERVATIONS_009_067

- Wind: http://mandeo.meteogalicia.es/thredds/catalogos/DATOS/ARCHIVE/WRF/WRF_hist.html

Acknowledgments

We thank the Emergencies and Meteorology Directorate (Security department) of the Basque Government for public data provision from the Basque Operational Oceanography System EuskOOS. This study has been conducted using EU Copernicus Marine Service information. Wind data were obtained from the meteorological agency of Galicia (Meteo-Galicia). The processing of HFR data was supported by JERICO-S3 project, funded by the European Union's Horizon 2020 Research and Innovation Program under grant agreement no. 871153. This study has also been undertaken with the financial support of the "Departamento de Medio Ambiente, Ordenación del Territorio, Agricultura y Pesca" of the Basque Government (MarcoProgram). This work has been done partially with financial support from the project LAMARCA (PID2021-123352OB-C31; PID2021-123352OB-C33) funded by MICIN/AEI /10.13039/501100011033/ and by FEDER (UE), the project Tech2Coast (TED2021-130949B-I00) funded by MCIN/AEI/ 10.13039/501100011033 and by EU "NextGenerationEU/PRTR" and the project EuroSea funded by he European Union's Horizon 2020 Research and Innovation Programme under grant agreement No.862626. This study is a contribution to the IM22MPDH project, funded by the EMFF (European Maritime Fishing Funds) Data collection framework, the "Departamento de Desarrollo Económico y Competitividad" of the Basque Government and the "Secretaría General de Pesca" of the Spanish Government providing the oceanographic vessels Emma Bardán. Ivan Manso-Narvarte was supported by a PhD fellowship from the "Departamento de Medio Ambiente, Ordenación del Territorio, Agricultura y Pesca" of the Basque Government. Ismael Hernández-Carrasco acknowledges financial support from the project TRITOP (grant\# UIB2021-PD06) funded by University of the Balearic Islands and by FEDER(EU). This is contribution number 1183 of the Marine Research Division of AZTI-BRTA.

Appendix A. Supplementary data

Supplementary data to this article can be found online at https://doi.org/10.1016/j.jmarsys.2023.103938.

References

Abascal, A.J., Castanedo, S., Medina, R., Liste, M., 2010. Analysis of the reliability of a statistical oil spill response model. Mar. Pollut. Bull. 60, 2099–2110. https://doi.org/10.1016/j.marpolbul.2010.07.008.

Aldanondo, N., Cotano, U., Etxebeste, E., Irigoien, X., Álvarez, P., de Murguía, A.M., Herrero, D.L., 2008. Validation of daily increments deposition in the otoliths of European anchovy larvae (*Engraulis encrasicolus* L.) reared under different temperature conditions. Fish. Res. 93, 257–264. https://doi.org/10.1016/j.fishres.2008.04.012.

Aldanondo, N., Cotano, U., Tiepolo, M., Boyra, G., Irigoien, X., 2010. Growth and movement patterns of early juvenile European anchovy (*Engraulis encrasicolus* L.) in the Bay of Biscay based on otolith microstructure and chemistry. Fish. Oceanogr. 19, 196–208. https://doi.org/10.1111/j.1365-2419.2010.00537.x.

Allain, G., Petitgas, P., Lazure, P., Grellier, P., 2001. The transport of anchovy larvae and juveniles across the Bay of Biscay studied using otolith increments and a 3D hydrodynamic model. ICES 1. C. 2001/W:01.

Allain, G., Petitgas, P., Lazure, P., 2007. The influence of environment and spawning distribution on the survival of anchovy (*Engraulis encrasicolus*) larvae in the Bay of Biscay (NE Atlantic) investigated by biophysical simulations. Fish. Oceanogr. 16, 506–514. https://doi.org/10.1111/j.1365-2419.2007.00442.x.

Bachiller, E., Cotano, U., Boyra, G., Irigoien, X., 2013. Spatial distribution of the stomach weights of juvenile anchovy (*Engraulis encrasicolus* L.) in the Bay of Biscay. ICES J. Mar. Sci. 70, 362–378. https://doi.org/10.1093/icesjms/fss176.

Bender, L.C., DiMarco, S.F., 2009. Quality Control Analysis of Acoustic Doppler Current Profiler Data Collected on Offshore Platforms of the Gulf of Mexico. New Orleans, LA.

Boffetta, G., Celani, A., Cencini, M., Lacorata, G., Vulpiani, A., 2000. Nonasymptotic properties of transport and mixing. Chaos: Interdiscip. J. Nonlinear Sci. 10, 50–60. https://doi.org/10.1063/1.166475.

Boyra, G., Rueda, L., Coombs, S.H., Sundby, S., Ådlandsvik, B., Santos, M., Uriarte, A., 2003. Modelling the vertical distribution of eggs of anchovy (*Engraulis encrasicolus*) and sardine (*Sardina pilchardus*). Fish. Oceanogr. 12, 381–395. https://doi.org/10.1046/j.1365-2419.2003.00260.x.

Boyra, G., Peña, M., Cotano, U., Irigoien, X., Rubio, A., Nogueira, E., 2016. Spatial dynamics of juvenile anchovy in the Bay of Biscay. Fish. Oceanogr. 25, 529–543. https://doi.org/10.1111/fog.12170.

Caballero, A., Pascual, A., Dibarboure, G., Espino, M., 2008. Sea level and eddy kinetic energy variability in the Bay of Biscay, inferred from satellite altimeter data. J. Mar. Syst. 72, 116–134. https://doi.org/10.1016/j.jmarsys.2007.03.011.

Caballero, A., Ferrer, L., Rubio, A., Charria, G., Taylor, B.H., Grima, N., 2014. Monitoring of a quasi-stationary eddy in the Bay of Biscay by means of satellite, in situ and model results. Deep-Sea Res. II Top. Stud. Oceanogr. 106, 23–37. https://doi.org/10.1016/j.dsr2.2013.09.029.

Caballero, A., Rubio, A., Ruiz, S., Le Cann, B., Testor, P., Mader, J., Hernández, C., 2016. South-Eastern Bay of Biscay eddy-induced anomalies and their effect on chlorophyll distribution. J. Mar. Syst. 162, 57–72. https://doi.org/10.1016/j.jmarsys.2016.04.001.

Campbell, R., Diaz, F., Hu, Z., Doglioli, A., Petrenko, A., Dekeyser, I., 2013. Nutrients and plankton spatial distributions induced by a coastal eddy in the Gulf of Lion. Insights from a numerical model. Prog. Oceanogr. 109, 47–69. https://doi.org/10.1016/j.pocean.2012.09.005.

Capó, E., McWilliams, J.C., Mason, E., Orfila, A., 2021. Intermittent frontogenesis in the Alboran Sea. J. Phys. Oceanogr. 51, 1417–1439. https://doi.org/10.1175/JPO-D-20-0277.1.

Charria, G., Lazure, P., Le Cann, B., Serpette, A., Reverdin, G., Louazel, S., Batifoulier, F., Dumas, F., Pichon, A., Morel, Y., 2013. Surface layer circulation derived from Lagrangian drifters in the Bay of Biscay. J. Mar. Syst. 109, S60–S76. https://doi.org/10.1016/j.jmarsys.2011.09.015.

Checkley, D.M., Ortner, P.B., Settle, L.R., Cummings, S.R., 1997. A continuous, underway fish egg sampler. Fish. Oceanogr. 6, 58–73. https://doi.org/10.1046/j.1365-2419.1997.00030.x.

Coombs, S.H., Boyra, G., Rueda, L.D., Uriarte, A., Santos, M., Conway, D.V.P., Halliday, N.C., 2004. Buoyancy measurements and vertical distribution of eggs of sardine (*Sardina pilchardus*) and anchovy (*Engraulis encrasicolus*). Mar. Biol. 145, 959–970. https://doi.org/10.1007/s00227-004-1389-4.

Cotano, U., Irigoien, X., Etxebeste, E., Álvarez, P., Zarauz, L., Mader, J., Ferrer, L., 2008. Distribution, growth and survival of anchovy larvae (*Engraulis encrasicolus* L.) in relation to hydrodynamic and trophic environment in the Bay of Biscay. J. Plankton Res. 30, 467–481. https://doi.org/10.1093/plankt/fbn011.

De Mey-Frémaux, P., Ayoub, N., Barth, A., Brewin, R., Charria, G., Campuzano, F., Ciavatta, S., Cirano, M., Edwards, C.A., Federico, I., Gao, S., Garcia-Hermosa, I., Garcia-Sotillo, M., Hewitt, H., Hole, L.R., Holt, J., King, R., Kourafalou, V., Lu, Y., Mourre, B., Pascual, A., Staneva, J., Stanev, E., Wang, H., Zhu, X., 2019. Model-observations synergy in the coastal ocean. Front. Mar. Sci. 6, 436.

Declerck, A., Delpey, M., Rubio, A., Ferrer, L., Basurko, O.C., Mader, J., Louzao, M., 2019. Transport of floating marine litter in the coastal area of the South-Eastern Bay of Biscay: a Lagrangian approach using modelling and observations. J. Oper. Oceanogr. 12, S111–S125. https://doi.org/10.1080/1755876X.2019.1611708.

Díaz-Barroso, L., Hernández-Carrasco, I., Orfila, A., Reglero, P., Balbín, R., Hidalgo, M., Tintoré, J., Alemany, F., Alvarez-Berastegui, D., 2022. Singularities of surface mixing activity in the Western Mediterranean influence bluefin tuna larval habitats. Mar. Ecol. Prog. Ser. 685, 69–84. https://doi.org/10.3354/meps13979.

d'Ovidio, F., Fernández, V., Hernández-García, E., López, C., 2004. Mixing structures in the Mediterranean Sea from finite-size Lyapunov exponents. Geophys. Res. Lett. 31 https://doi.org/10.1029/2004GL020328.

Edwards, K.P., Hare, J.A., Werner, F.E., Seim, H., 2007. Using 2-dimensional dispersal kernels to identify the dominant influences on larval dispersal on continental shelves. Mar. Ecol. Prog. Ser. 352, 77–87. https://doi.org/10.3354/meps07169.

Ferrer, L., González, M., Cotano, U., Uriarte, A., Sagarminaga, Y., Santos, M., Uriarte, Ad, Collins, M., 2004. Physical controls on the evolution of anchovy in the Bay of Biscay: a numerical approximation. In: ICES Ann. Sci. Conf. Vigo, p. 20.

Ferrer, L., Liria, P., Bolaños, R., Balseiro, C., Carracedo, P., González-Marco, D., González, M., Fontán, A., Mader, J., Hernández, C., 2010. Reliability of coupled meteorological and wave models to estimate wave energy resource in the Bay of Biscay. In: Proceedings of the 3rd International Conference on Ocean Energy (ICOE). Bilbao (Spain), pp. 6–8.

Garcia-Soto, C., Pingree, R.D., Valdés, L., 2002. Navidad development in the southern Bay of Biscay: climate change and swoddy structure from remote sensing and in situ measurements. J. Geophys. Res. Oceans 107, 28-1-28–29.

Garden, C.J., Currie, K., Fraser, C.I., Waters, J.M., 2014. Rafting dispersal constrained by an oceanographic boundary. Mar. Ecol. Prog. Ser. 501, 297–302. https://doi.org/10.3354/meps10675.

González, M., Uriarte, A., Fontán, A., Mader, J., Gyssels, P., 2004. Marine dynamics. Oceanogr. Mar. Environ. Basque Country 70, 133–157.

Haller, G., 2015. Lagrangian coherent structures. Annu. Rev. Fluid Mech. 47, 137–162. https://doi.org/10.1146/annurev-fluid-010313-141322.

Haller, G., Yuan, G., 2000. Lagrangian coherent structures and mixing in two-dimensional turbulence. Phys. D: Nonlinear Phenom. 147, 352–370. https://doi.org/10.1016/S0167-2789(00)00142-1.

Hernández-Carrasco, I., Orfila, A., 2018. The role of an intense front on the connectivity of the Western Mediterranean Sea: the Cartagena-Tenes front. J. Geophys. Res. Oceans 123, 4398–4422. https://doi.org/10.1029/2017JC013613.

Hernández-Carrasco, I., López, C., Hernández-García, E., Turiel, A., 2011. How reliable are finite-size Lyapunov exponents for the assessment of ocean dynamics? Ocean Model 36, 208–218. https://doi.org/10.1016/j.ocemod.2010.12.006.

Hernández-Carrasco, I., Orfila, A., Rossi, V., Garçon, V., 2018a. Effect of small scale transport processes on phytoplankton distribution in coastal seas. Sci. Rep. 8, 1–13. https://doi.org/10.1038/s41598-018-26857-9.

Hernández-Carrasco, I., Solabarrieta, L., Rubio, A., Esnaola, G., Reyes, E., Orfila, A., 2018b. Impact of HF radar current gap-filling methodologies on the Lagrangian assessment of coastal dynamics. Ocean Sci. 14, 827–847. https://doi.org/10.5194/os-14-827-2018.

Hidalgo, M., Rossi, V., Monroy, P., Ser-Giacomi, E., Hernández-García, E., Guijarro, B., Massutí, E., Alemany, F., Jadaud, A., Perez, J.L., 2019. Accounting for ocean connectivity and hydroclimate in fish recruitment fluctuations within transboundary metapopulations. Ecol. Appl. 29, e01913 https://doi.org/10.1002/eap.1913.

Huret, M., Petitgas, P., Woillez, M., 2010. Dispersal kernels and their drivers captured with a hydrodynamic model and spatial indices: a case study on anchovy (*Engraulis encrasicolus*) early life stages in the Bay of Biscay. Prog. Oceanogr. 87, 6–17. https://doi.org/10.1016/j.pocean.2010.09.023.

Irigoien, X., Cotano, U., Boyra, G., Santos, M., Alvarez, P., Otheguy, P., Etxebeste, E., Uriarte, A., Ferrer, L., Ibaibarriaga, L., 2008. From egg to juvenile in the Bay of Biscay: spatial patterns of anchovy (*Engraulis encrasicolus*) recruitment in a non-upwelling region. Fish. Oceanogr. 17, 446–462. https://doi.org/10.1111/j.1365-2419.2008.00492.x.

Jordà, G., Sánchez-Román, A., Gomis, D., 2016. Reconstruction of transports through the Strait of Gibraltar from limited observations. Clim. Dyn. 48, 851–865. https://doi.org/10.1007/s00382-016-3113-8.

Kaplan, D.M., Lekien, F., 2007. Spatial interpolation and filtering of surface current data based on open-boundary modal analysis. J. Geophys. Res. Oceans 112. https://doi.org/10.1029/2006JC003984.

Kaplan, A., Kushnir, Y., Cane, M.A., Blumenthal, M.B., 1997. Reduced space optimal analysis for historical data sets: 136 years of Atlantic sea surface temperatures. J. Geophys. Res. Oceans 102, 27835–27860. https://doi.org/10.1029/97JC01734.

Lehahn, Y., D'Ovidio, F., Lévy, M., Heifetz, E., 2007. Stirring of the Northeast Atlantic spring bloom: a Lagrangian analysis based on multisatellite data. J. Geophys. Res. Oceans 112. https://doi.org/10.1029/2006JC003927.

Leitão, P.C., 1996. Modelo de dispersão lagrangeano tridimensional. Technical University of Lisbon.

Manso-Narvarte, I., Fredj, E., Jordà, G., Berta, M., Griffa, A., Caballero, A., Rubio, A., 2020. 3D reconstruction of ocean velocity from high-frequency radar and acoustic Doppler current profiler: a model-based assessment study. Ocean Sci. 16, 575–591. https://doi.org/10.5194/os-16-575-2020.

Manso-Narvarte, I., Rubio, A., Jordà, G., Carpenter, J., Merckelbach, L., Caballero, A., 2021. Three-dimensional characterization of a coastal mode-water eddy from multiplatform observations and a data reconstruction method. Remote Sens. 13, 674. https://doi.org/10.3390/rs13040674.

Mantovani, C., Corgnati, L., Horstmann, J., Rubio, A., Reyes, E., Quentin, C., Cosoli, S., Asensio, J.L., Mader, J., Griffa, A., 2020. Best practices on high frequency radar deployment and operation for ocean current measurement. Front. Mar. Sci. 7, 210. https://doi.org/10.3389/fmars.2020.00210.

Moore, T.S., Matear, R.J., Marra, J., Clementson, L., 2007. Phytoplankton variability off the Western Australian coast: mesoscale eddies and their role in cross-shelf exchange. Deep-Sea Res. II Top. Stud. Oceanogr. 54, 943–960. https://doi.org/10.1016/j.dsr2.2007.02.006.

Moser, H.G., Ahlstrom, E.H., 1985. Staging anchovy eggs. NOAA Tech. Rep. NMFS 36, 37–41.

Motos, L., Uriarte, A., Valencia, V., 1996. The spawning environment of the Bay of Biscay anchovy (*Engraulis encrasicolus* L.). Sci. Mar. 60, 117–140.

Mullaney, T.J., Suthers, I.M., 2013. Entrainment and retention of the coastal larval fish assemblage by a short-lived, submesoscale, frontal eddy of the East Australian Current. Limnol. Oceanogr. 58, 1546–1556. https://doi.org/10.4319/lo.2013.58.5.1546.

Neves, R., 2013. The MOHID concept. In: Neves, R., Mateus, M. (Eds.), Ocean Modelling for Coastal Management-Case Studies with MOHID. IST Press, Lisbon, pp. 1–11.

Okubo, A., 1971. Oceanic diffusion diagrams. In: Deep Sea Research and Oceanographic Abstracts. Elsevier, pp. 789–802.

Olivar, M.P., Salat, J., Palomera, I., 2001. Comparative study of spatial distribution patterns of the early stages of anchovy and pilchard in the NW Mediterranean Sea. Mar. Ecol. Prog. Ser. 217, 111–120. https://doi.org/10.3354/meps217111.

OSPAR, 2000. Quality status report 2000: region IV-Bay of Biscay and Iberian coast. In: OSPAR Commission for the Protection of the Marine Environment of the North-East Atlantic, London.

Ospina-Alvarez, A., Parada, C., Palomera, I., 2012. Vertical migration effects on the dispersion and recruitment of European anchovy larvae: from spawning to nursery areas. Ecol. Model. 231, 65–79. https://doi.org/10.1016/j.ecolmodel.2012.02.001.

Otero, P., Ruiz-Villarreal, M., Allen-Perkins, S., Vila, B., Cabanas, J.M., 2014. Coastal exposure to oil spill impacts from the Finisterre traffic separation scheme. Mar. Pollut. Bull. 85, 67–77. https://doi.org/10.1016/j.marpolbul.2014.06.020.

Palatella, L., Bignami, F., Falcini, F., Lacorata, G., Lanotte, A.S., Santoleri, R., 2014. Lagrangian simulations and interannual variability of anchovy egg and larva dispersal in the Sicily Channel. J. Geophys. Res. Oceans 119, 1306–1323. https://doi.org/10.1002/2013JC009384.

Palomera, I., 1991. Vertical distribution of anchovy larvae *Engraulis encrasicolus* in Western Mediterranean. ICES C 50, 31.

Parada, C., Mullon, C., Roy, C., Fréon, P., Hutchings, L., Van der Lingen, C.D., 2008. Does vertical migratory behaviour retain fish larvae onshore in upwelling ecosystems? A modelling study of anchovy in the southern Benguela. Afr. J. Mar. Sci. 30, 437–452. https://doi.org/10.2989/AJMS.2008.30.3.1.635.

Pingree, R.D., Le Cann, B., 1992a. Three anticyclonic slope water oceanic eDDIES (SWODDIES) in the southern Bay of Biscay in 1990. Deep Sea Res. A: Oceanogr. Res. Pap. 39, 1147–1175. https://doi.org/10.1016/0198-0149(92)90062-X.

Pingree, R.D., Le Cann, B., 1992b. Anticyclonic eddy X91 in the southern Bay of Biscay, May 1991 to February 1992. J. Geophys. Res. Oceans 97, 14353–14367. https://doi.org/10.1029/92JC01181.

Reyes, E., Aguiar, E., Bendoni, M., Berta, M., Brandini, C., Cáceres-Euse, A., Capodici, F., Cardin, V., Cianelli, D., Ciraolo, G., 2022. Coastal high-frequency radars in the Mediterranean–Part 2: applications in support of science priorities and societal needs. Ocean Sci. 18, 797–837. https://doi.org/10.5194/os-18-797-2022.

Roarty, H., Cook, T., Hazard, L., Harlan, J., Cosoli, S., Wyatt, L., Alvarez Fanjul, E., Terrill, E., Otero, M., Largier, J., 2019. The global high frequency radar network. Front. Mar. Sci. 6, 164.

Rodríguez, J.M., Barton, E.D., Hernández-León, S., Arístegui, J., 2004. The influence of mesoscale physical processes on the larval fish community in the Canaries CTZ, in summer. Prog. Oceanogr. 62, 171–188. https://doi.org/10.1016/j.pocean.2004.07.006.

Rubio, A., Reverdin, G., Fontán, A., González, M., Mader, J., 2011. Mapping near-inertial variability in the SE Bay of Biscay from HF radar data and two offshore moored buoys. Geophys. Res. Lett. 38 https://doi.org/10.1029/2011GL048783.

Rubio, A., Solabarrieta, L., González, M., Mader, J., Castanedo, S., Medina, R., Charria, G., Aranda, J.A., 2013. Surface circulation and Lagrangian transport in the SE Bay of Biscay from HF radar data. In: 2013 MTS/IEEE OCEANS-Bergen. IEEE, pp. 1–7. https://doi.org/10.1109/OCEANS-Bergen.2013.6608039.

Rubio, A., Mader, J., Corgnati, L., Mantovani, C., Griffa, A., Novellino, A., Quentin, C., Wyatt, L., Schulz-Stellenfleth, J., Horstmann, J., 2017. HF radar activity in European coastal seas: next steps toward a pan-European HF radar network. Front. Mar. Sci. 4, 8. https://doi.org/10.3389/fmars.2017.00008.

Rubio, A., Caballero, A., Orfila, A., Hernández-Carrasco, I., Ferrer, L., González, M., Solabarrieta, L., Mader, J., 2018. Eddy-induced cross-shelf export of high Chl-a coastal waters in the SE Bay of Biscay. Remote Sens. Environ. 205, 290–304. https://doi.org/10.1016/j.rse.2017.10.037.

Rubio, A., Manso-Narvarte, I., Caballero, A., Corgnati, L., Mantovani, C., Reyes, E., Griffa, A., Mader, J., 2019. The seasonal intensification of the slope Iberian Poleward Current. In: Copernicus Marine Service Ocean State Report. J. Oper. Oceanogr, 3, pp. 13–18. https://doi.org/10.1080/1755876X.2019.1633075.

Rubio, A., Hernández-Carrasco, I., Orfila, A., González, M., Reyes, E., Corgnati, L., Berta, M., Griffa, A., Mader, J., 2020. A lagrangian approach to monitor local particle retention conditions in coastal areas. In: Copernicus Marine Service Ocean State Report. J. Oper. Ocean, 13, pp. 10–1080. https://doi.org/10.1080/1755876X.2020.1785097.

Ruiz, I., Basurko, O.C., Rubio, A., Delpey, M., Granado, I., Declerck, A., Mader, J., Cózar-Cabañas, A., 2020. Litter windrows in the south-east coast of the Bay of Biscay: an ocean process enabling effective active fishing for litter. Front. Mar. Sci. 7, 308. https://doi.org/10.3389/fmars.2020.00308.

Sabatés, A., Olivar, M.P., Salat, J., Palomera, I., Alemany, F., 2007a. Physical and biological processes controlling the distribution of fish larvae in the NW Mediterranean. Prog. Oceanogr. 74, 355–376. https://doi.org/10.1016/j.pocean.2007.04.017.

Sabatés, A., Salat, J., Palomera, I., Emelianov, M., Fernández de Puelles, M.L., Olivar, M. P., 2007b. Advection of anchovy (*Engraulis encrasicolus*) larvae along the Catalan continental slope (NW Mediterranean). Fish. Oceanogr. 16, 130–141. https://doi.org/10.1111/j.1365-2419.2006.00416.x.

Santos, M., Uriarte, A., Ibaibarriaga, L., 2011. Spawning stock biomass estimates of the Bay of Biscay anchovy (*Engraulis encrasicolus*, L.) in 2010 applying the daily egg production method. Rev. Investig. Mar. (Mar. Res. J.) 18, 76–91.

Sciascia, R., Berta, M., Carlson, D.F., Griffa, A., Panfili, M., La Mesa, M., Corgnati, L., Mantovani, C., Domenella, E., Fredj, E., 2018. Linking sardine recruitment in coastal areas to ocean currents using surface drifters and HF radar: a case study in the Gulf of Manfredonia, Adriatic Sea. Ocean Sci. 14, 1461–1482. https://doi.org/10.5194/os-14-1461-2018.

Sebastiao, P., Soares, C.G., 2006. Uncertainty in predictions of oil spill trajectories in a coastal zone. J. Mar. Syst. 63, 257–269. https://doi.org/10.1016/j.jmarsys.2006.06.002.

Shadden, S.C., Lekien, F., Paduan, J.D., Chavez, F.P., Marsden, J.E., 2009. The correlation between surface drifters and coherent structures based on high-frequency radar data in Monterey Bay. Deep-Sea Res. II Top. Stud. Oceanogr. 56, 161–172. https://doi.org/10.1016/j.dsr2.2008.08.008.

Smith, P.E., Flerx, W., Hewitt, R.P., 1985. The CalCOFI vertical egg tow (CalVET) net. In: Lasker, R. (Ed.), An Egg Production Method for Estimating Spawning Biomass of Pelagic Fish: Application to the Northern Anchoy (*Engraulis Mordax*). US Department of Commerce NOAA Tech. Rep., pp. 27–32

Solabarrieta, L., Rubio, A., Castanedo, S., Medina, R., Charria, G., Hernández, C., 2014. Surface water circulation patterns in the southeastern Bay of Biscay: new evidences from HF radar data. Cont. Shelf Res. 74, 60–76. https://doi.org/10.1016/j.csr.2013.11.022.

Solabarrieta, L., Rubio, A., Cárdenas, M., Castanedo, S., Esnaola, G., Méndez, F.J., Medina, R., Ferrer, L., 2015. Probabilistic relationships between wind and surface water circulation patterns in the SE Bay of Biscay. Ocean Dyn. 65, 1289–1303. https://doi.org/10.1007/s10236-015-0871-5.

Solabarrieta, L., Frolov, S., Cook, M., Paduan, J., Rubio, A., González, M., Mader, J., Charria, G., 2016. Skill assessment of HF radar–derived products for lagrangian simulations in the Bay of Biscay. J. Atmos. Ocean. Technol. 33, 2585–2597. https://doi.org/10.1175/JTECH-D-16-0045.1.

Somarakis, S., Nikolioudakis, N., 2007. Oceanographic habitat, growth and mortality of larval anchovy (*Engraulis encrasicolus*) in the northern Aegean Sea (eastern

Mediterranean). Mar. Biol. 152, 1143–1158. https://doi.org/10.1007/s00227-007-0761-6.

Sotillo, M.G., Cailleau, S., Lorente, P., Levier, B., Aznar, R., Reffray, G., Amo-Baladrón, A., Chanut, J., Benkiran, M., Alvarez-Fanjul, E., 2015. The MyOcean IBI Ocean forecast and reanalysis systems: operational products and roadmap to the future Copernicus service. J. Oper. Oceanogr. 8, 63–79. https://doi.org/10.1080/1755876X.2015.1014663.

Tarry, D.R., Ruiz, S., Johnston, T.M.S., Poulain, P., Özgökmen, T., Centurioni, L.R., Berta, M., Esposito, G., Farrar, J.T., Mahadevan, A., 2022. Drifter observations reveal intense vertical velocity in a surface ocean front. Geophys. Res. Lett. 49 https://doi.org/10.1029/2020JC016614 e2022GL098969.

Uriarte, A., Sagarminaga, Y., Scalabrin, C., Valencia, V., Cermeño, P., De Miguel, E., Gómez Sánchez, J.A., Jiménez, M., 2001. Ecology of anchovy juveniles in the Bay of Biscay 4 months after peak spawning: do they form part of the plankton. ICES CM W: 20, 1–45.

Van Sebille, E., Aliani, S., Law, K.L., Maximenko, N., Alsina, J.M., Bagaev, A., Bergmann, M., Chapron, B., Chubarenko, I., Cózar, A., Delandmeter, P., Egger, M., Fox-Kemper, B., Garaba, P.S., Lonneke, G.-M., Hardesty, B.D., Hoffman, M.J., Isobe, A., Jongedijk, C.E., Kaandorp, M.L.A., Khatmullina, L., Koelmans, A.A., Kukulka, T., Laufkötter, C., Lebreton, L., Lobelle, D., Maes, C., Martinez-Vicente, V., Morales Maqueda, M.A., Poulain-Zarcos, M., Rodríguez, E., Ryan, P.G., Shanks, A.L., Shim, W.J., Suaria, G., Thiel, M., van den Bremer, T.S., Wichmann, D., 2020. The physical oceanography of the transport of floating marine debris. Environ. Res. Lett. 15, 23003. https://doi.org/10.1088/1748-9326/ab6d7d.